

AN ABSTRACT OF THE THESIS OF

Congcong Hu for the degree of Master of Science in Materials Science presented on June 19, 2014

Title: Simulations of Geckos Dry Adhesion System

Abstract approved:

P. Alex Greaney

Simulation models were developed to explore the reversible nature of gecko dry adhesion system. The central idea of this model is that even with a small moment imparted on the contact tip, the seta can be easily ad-adhered. It is shown that this contact condition is very sensitive, but can result in robust adhesion if individual seta is canted and highly flexible. In analogy to the “cone of friction”, we consider the “area of adhesion” — the domain of normal and tangential forces that maintain adhesion. Results demonstrate that this adhesion region is highly asymmetric enabling the gecko to adhere under a variety of loading conditions associated with scuttling horizontally, vertically and inverted. Moreover, under each of these conditions there is a low energy path to de-adhesion. In this model obliquely canted seta (as possessed by geckos) rather than vertically aligned fibers (common in synthetic dry adhesive) provide the most robust adhesion.

©Copyright by Congcong Hu
June 19, 2014
All Rights Reserved

Simulations of Geckos Dry Adhesion System

by

Congcong Hu

A THESIS

submitted to

Oregon State University

in partial fulfillment of
the requirements for the
degree of

Master of Science

Presented June 19, 2014

Commencement June 2015

Master of Science thesis of Congcong Hu presented on June 19, 2014

APPROVED:

Major Professor, representing Materials Science

Director of the Materials Science Program

Dean of the Graduate School

I understand that my thesis will become part of the permanent collection of Oregon State University libraries. My signature below authorizes release of my thesis to any reader upon request.

Congcong Hu, Author

ACKNOWLEDGEMENTS

I could not have completed this research without assistance from many people. The people listed below are those who contributed directly to this thesis, but many other people have helped me along the way. I thank you all for making my experience at OSU great.

In particular, I would like to express many thanks to my main advisor, Dr. Alex Greaney, for his guidance and support throughout my research. I would not make it without his encouragement and patience. Also, many other faculty members at Materials Science department have helped me along the way. Thanks to Dr. Bill Warnes and Dr. David Cann for getting me onto the right track of graduate program. Thanks also to my thesis committee members, including Dr. Solomon Yim and Dr. David Hackleman, for their participation and valuable suggestions.

Special recognition is necessary for my coworkers, especially Saranam Venkata Rajesh, Laura Oliveira and Luping Han. They have never failed to offer a helping hand, share their knowledge, and suggest good ideas. I cannot thank them enough.

Finally, thanks to my families. I could not get this far without their support.

Sincerely,

Congcong Hu

CONTRIBUTION OF AUTHORS

Dr. Alex Greaney helped in many aspects of this work including technical support, making suggestions on simulation methods and data analysis. He also helped with reviewing and revising the manuscript and this thesis.

TABLE OF CONTENTS

| | <u>Page</u> |
|--|-------------|
| 1 Introduction | 1 |
| 1.1 General Introduction | 1 |
| 1.2 History | 2 |
| 1.3 Primary Mechanism | 3 |
| 1.4 Gecko-inspired Synthetic Adhesives | 5 |
| 1.5 Computational Models for Gecko Adhesion..... | 8 |
| 1.6 References | 11 |
| 2 Background Theory | 14 |
| 2.1 Microscopic/Hamaker Approach | 14 |
| 2.2 Gecko Adhesion Forces | 16 |
| 2.3 Cohesive Contact Assumption in This Study..... | 18 |
| 2.4 References | 19 |
| 3 Manuscript | 20 |
| 3.1 Abstract | 21 |
| 3.2 Introduction | 21 |
| 3.3 Heuristic Model..... | 23 |
| 3.3.1 Moment-supporting Contact | 23 |
| 3.3.2 Flexible Seta..... | 27 |
| 3.4 Gecko Model..... | 33 |
| 3.4.1 Gecko Model Setup..... | 33 |
| 3.4.2 Gecko Model: Results and Discussion..... | 36 |
| 3.5 Conclusions | 43 |

TABLE OF CONTENTS

| | <u>Page</u> |
|--------------------------|-------------|
| 3.6 Acknowledgments..... | 44 |
| 3.7 References..... | 44 |
| 4 Conclusion..... | 47 |

LIST OF FIGURES

| <u>Figure</u> | <u>Page</u> |
|--|-------------|
| 1.1 Pictures of a moving gecko captured by high speed cameras. (<i>Mongeau et al. 2012</i>) | 1 |
| 1.2 Enlarged picture of an individual seta (<i>Autumn 2006</i>) | 4 |
| 1.3 Multiple kinds of synthetic adhesives (<i>Lee et al. 2008, Ge et al. 2007, Jeong et al. 2009, Tamelier et al. 2012</i>)..... | 7 |
| 1.4 Several computational models for gecko setae (<i>Bhushan 2007, Lee 2008, Takahashi 2006</i>)..... | 10 |
| 2.1 Force response curve..... | 14 |
| 2.2 Interaction between a molecule and an infinite solid (<i>Butt et al. 2010</i>) | 15 |
| 2.3 Cohesive between seta tips and flat surface..... | 18 |
| 3.1 Heuristic model and adhesion criterion | 24 |
| 3.2 Adhesion region and robustness plots..... | 29 |
| 3.3 Schematic contrasting geckos' dry adhesion with static friction..... | 30 |
| 3.4 Plot of the adhesion region for seta with nonlinear bending stiffness overlaid with the adhesion region for linear seta | 32 |
| 3.5 Gecko model | 35 |
| 3.6 Plots of the adhesion region of the two-torsional-spring model..... | 41 |
| 3.7 Density maps of the stored elastic energy in a seta | 42 |

1 INTRODUCTION

1.1 GENERAL INTRODUCTION

1,500 different species of geckos are found worldwide, and many of them are well known as the strongest climbers in nature. They can climb completely upright, vertically, or even upside-down upon almost any material with various roughnesses. More than that, pictures taken by high speed cameras, as shown in Figure 1.1, show that geckos are able to run at up to twenty times their body length per second while adhering [1].



Figure 1.1: Pictures of a moving gecko captured by high speed cameras. (*Mongeau et al. 2012*)

Illustrated by Autumn as a specific example, a tokay gecko can produce 5 newtons adhesive force per foot, which is surprisingly large comparing to its weight (43 grams), but manages to lift the foot in just 15 milliseconds [2]. All these amazing skills need extremely well developed dry adhesion system that includes significantly high reversibility and controllability, also called *smart adhesion*. Here reversibility means the ability that enables geckos to de-adhere easily and quickly from the strong adhesion force, and controllability is the ability that adapts geckos to multiple

environments and conditions such as various surface roughnesses, adhering status (climbing, hanging, walking), *etc.* These novel characteristics make the geckos' dry adhesion system as a research topic with enduring popularity.

1.2 HISTORY

First commented on by Aristotle, determining how geckos adhere to a surface has been a challenging topic of scientific research for over a century. Many hypotheses have been proposed to explain the mechanism behind geckos' amazing climbing ability, including theories of glue, suction, electrostatics, friction and micro-interlocking, *etc* [3, 4]. The idea of sticky secretions was first proposed in 1830 but quickly eliminated. In this case, dry adhesion was proved since people found no glandular tissues on geckos' toes. The next idea that each seta acts as a tiny suction cup was first proposed in insect adhesion literature in 1845. However, no specific evidence was provided to support the suction theory, and Dellit (1934) suggested that suction was not involved in the adhesion process based on the results of adhesion experiments in a vacuum. Another idea of electrostatic attractive force between the setae and the surface was also proved invalid since experiments using X-ray bombardment (1934) showed that geckos were still able to adhere in ionized air. The theories of friction (1923) and micro-interlocking (1941) both suggested that the geometry of the surface plays an important role in the adhesion process. However, the theory of friction was easily ruled out since friction only operates parallel to the plane of contact but geckos need a strong vertical force component to support their weight when adhering to a ceiling. On the other hand, the theory of micro-interlocking, which claimed that the curved setae act like micro-scaled grappling hooks that can

attach to the irregularities of the rough surface, was also proved invalid according to adhesion tests on polished glass (1968) and recent tests on a molecular smooth SiO₂ semiconductor (2000). These experiments showed that a surface with high irregularity is not necessary for the generation of large adhesion force. Autumn et al. concluded that, in the geckos' case, the adhesion phenomenon is a result of molecular interaction rather than mechanical interlocking [4]. This conclusion is also consistent with the fact that geckos can climb on almost all materials with various surface conditions.

1.3 PRIMARY MECHANISM

The primary mechanism behind geckos' amazing climbing ability remained unknown for centuries until it was revealed by the development of Electron Microscope Science (EMS). In the early 1900s, scientists used light microscopes to observe that the underside of the gecko toe bears a series of *lamellae* structures, which are uniformly covered with millions of branched setae. In the 1960s, enlarged pictures taken by the electron microscope further revealed hundreds of split ends with flat tip structure, called the *spatulae*, on each individual seta. All these together construct the geckos' adhesion system as a hierarchical structure as illustrated in Figure 1.2. According to the study of Irschick et al., the pad area of a *tokay* gecko's two front feet is approximately 227 mm² and contains roughly 14,400 setae per square millimeter [5], and the dimension of an individual seta of a *tokay* gecko is approximately 110 micrometers long and 4.2 micrometers wide [2].

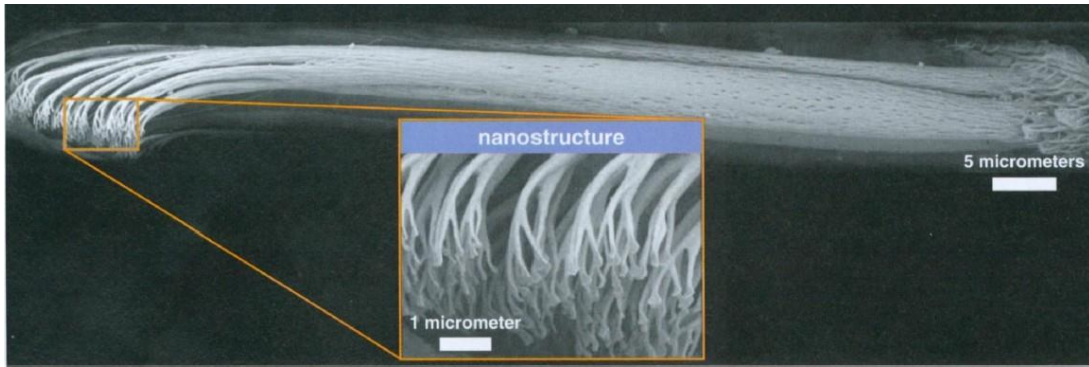


Figure 1.2: Enlarged picture of an individual seta. The dimension is measured as 110 micrometers long and 4.2 micrometers wide. (*Autumn, 2006*)

Even though the detailed structure of geckos' setae was well demonstrated, the main intermolecular mechanism between setae and their contacting surfaces still remained controversial during that time. Two potential intermolecular mechanisms, van der Waals force and capillary force, were suggested by Autumn et al. [4]. A series of adhesion experiments using a MEMS sensor were carried out later on to measure the normal and shear forces between setae and different surfaces with different polarities and hydrophobicities. It was shown that the remarkable adhesion ability of gecko setae is merely geometry and structure dependent, and is not affected by surface chemistry properties [4]. On the other hand, computational predicted results also verified that the computed structure based on van der Waals mechanism has similar dimension as real gecko setae [3]. Based on these cogent results, Autumn et al. announced in 2002 that the primary intermolecular mechanism in the geckos' adhesion process is van der Waals force. Currently, van der Waals force is generally accepted as the main molecular attractive force between the micro- or nano-scaled setae and the surface they are clinging to. Researches have shown that with the

hierarchical structure, geckos are able to maximize the contact area on either smooth or fractally rough surfaces, and enable robust load sharing [6, 7]. From a biomimetic point of view, geckos provide a template for efficient synthetic dry adhesion materials that include the characteristics of self-cleaning, adaptability and smart adhesion.

1.4 GECKO-INSPIRED SYNTHETIC ADHESIVES

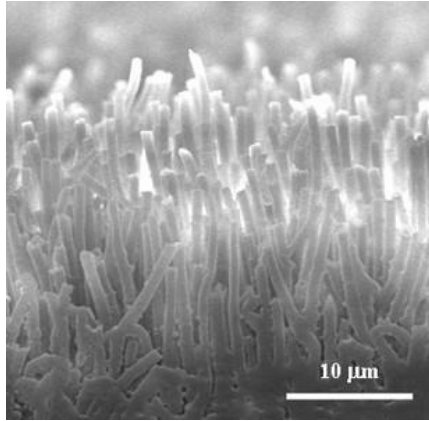
Inspired by the geckos' fibrillar structure, numerous groups have sought to create synthetic dry-adhesive tapes patterned with arrays of compliant micro-fibers or free-standing pillars that can replicate the phenomenon. Several initial attempts fabricated symmetrical synthetic fibers or pillars in vertical direction, such as hard polypropylene microfibers (Figure 1.3(a)) developed by Lee et al. [8] and multi-walled carbon nanotube setae (Figure 1.3(b)) developed by Ge et al. [9]. Tests results show that such synthetic dry-adhesives were able to support a large shear force when they slid on smooth substrates since a greater load causes more synthetic setae to engage, which increases the area of contact. From experiments [2] a *tokay* gecko is able to support 20.1 newtons shear force with its 227 square millimeter pad area, which is 8.85 N/cm², while most of these adhesives can produce approximate 10 N/cm². Additionally, these adhesives can be easily peeled if the shear load is removed.

With further studies identifying anisotropy as a key feature that is necessary for smart and reversible adhesion [10, 11], it is believed that the asymmetry in setae structures is a potential explanation for the high reversibility and controllability in geckos' adhesion system. Motivated by this, the latest generations of synthetic adhesives have explored a variety of strategies to create systematic anisotropy using different

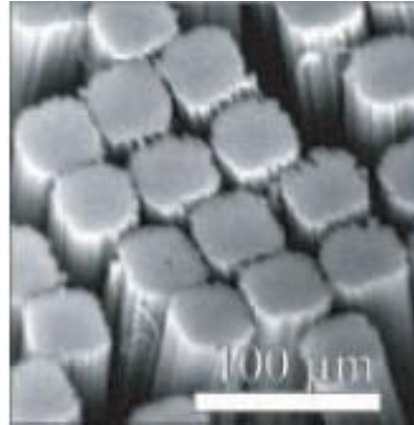
fabrication technics. These include presetting fibers or pillars with canted angles (Figure 1.3(c)), using hybrid materials and modifying the tip shape of symmetrical vertical microfibers (Figure 1.3(d)) [12-16]. It is not surprising to see that all those asymmetrical adhesives show enhancements in shear adhesion force when compared to those with symmetrical vertical fibers. The loads these asymmetric adhesives can support can go up to 20 N/cm^2 as shear force or even higher. Moreover, strong sticking and rapid peeling were defined as smart behaviors.

Although many of them have shown great performance in shear force testing, these applications are limited to some specific conditions, and these synthetic adhesives are still vastly outperformed by geckos themselves. On one hand, all these experiments and measurements are carried out under ideal testing conditions. Smooth substrates such as glass or PPMA (polymethyl methacrylate) were chosen to ensure good contact area. Testing samples are placed on to the surface carefully and loads are added slowly. No impact or any interference could be tolerated. In contrast, geckos developed their adhesion systems with such high robustness that enables them to adapt to far more complex natural environments. On the other hand, those current adhesives only exhibited one or two desirable properties, ie. generally most of these works focused on generating large shear force under applied normal load, but no comprehensive one like gecko's was reported. For instance, in ref [14], the fabricated adhesive with angled fibers showed little advantage in adhesion force over the one with vertical fibers. In ref [15], relatively large shear force was reported but no normal adhesion force was found. Overall, there is still a long path for synthetic

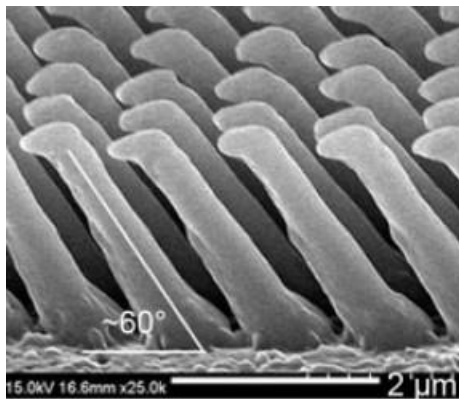
adhesives to match the performance of geckos.



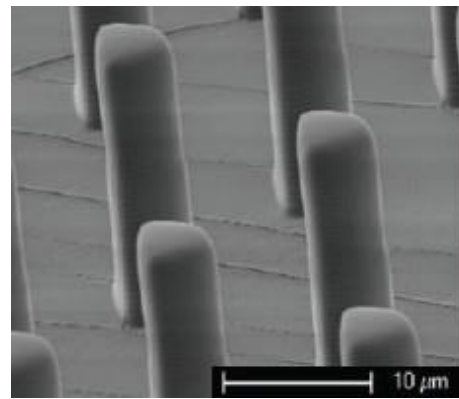
(a) Hard polypropylene microfibers (*Lee et al. 2008*)



(b) Multi-walled carbon nanotube setae (*Ge et al. 2007*)



(c) Fibers with canted angles (*Jeong et al. 2009*)



(d) Symmetrical vertical microfibers with tips shape modified (*Tamelier et al. 2012*)

Figure 1.3: Multiple kinds of synthetic adhesives.

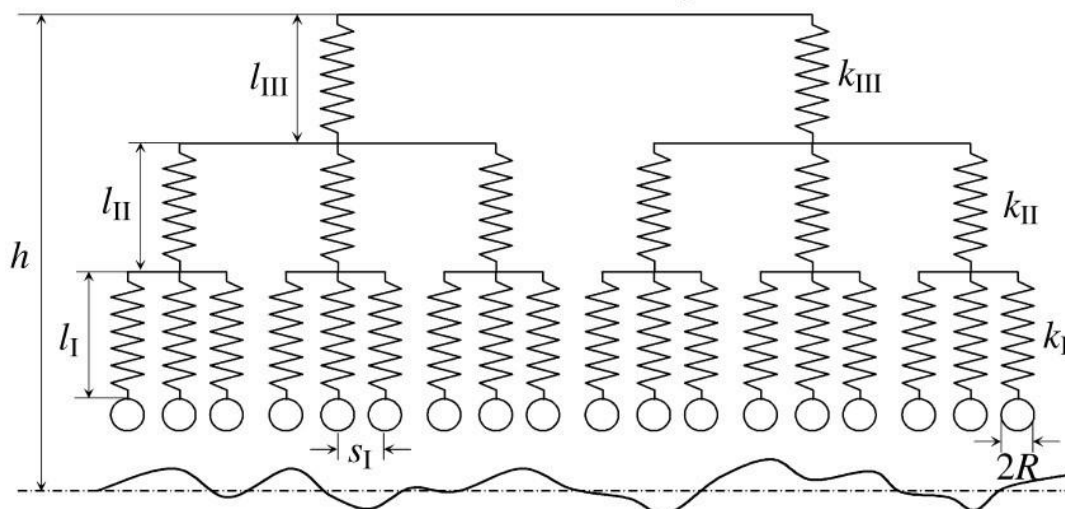
1.5 COMPUTATIONAL MODELS OF GECKO ADHESION

Due to the difficulty in exactly replicating geckos' adhesion system through fabrication, simplified computational models that contain potential influencing factors would be helpful in understanding the operation of such systems. Since the mechanism behind gecko adhesion is van der Waals force, geometric characteristics such as hierarchical structure, contact surface, oblique angle between seta and the contact surface, and the bending effect would be worthy to pay attention to, and it is believed that all those factors work synergistically to make the gecko adhesion system efficient and smart. A number of computational models have been powerful in understanding the difference between real gecko setae and synthetic adhesives. In general, these models can be divided into two categories: one pays attention to multiple setae that would form a hierarchical structure, and the other one focuses on single seta structure that would bend, buckle, extend or compress when responding to the adhesion process.

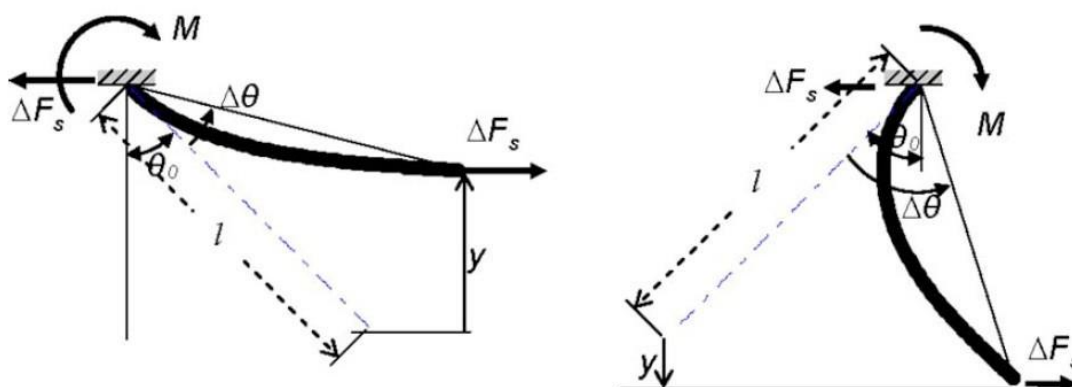
A simplified simulation model developed by Bhushan was the first study on the effect of hierarchical structure, and it used multiple discrete linear springs to simulate the hierarchical structure that geckos developed on their toes. In his simulation, Bhushan used the Derjaguin-Muller-Toporov (DMT) theory to calculate the adhesion force between setae and their contacting rough surfaces. Each seta can then be simplified to a linear spring with constant extension stiffness, suffering displacement normal to the rough surface. It was also very instructive that Bhushan introduced in his paper the way to evaluate simulated random rough surfaces with two performance parameters.

Through evaluating root mean square (RMS) amplitude and correlation length (CL), those simulated surfaces were created properly comparing with surfaces in reality. Two-level hierarchical structure was first analyzed [16] and was further extended to three-level hierarchy later on [6, 7], as shown in Figure 1.4(a). According to his simulation results, Bhushan commented that the hierarchical structure well explains the adhesion enhancements due to the increase in the area of contact, and it also contributes to geckos' ability of clinging to both smooth and rough surfaces. However, no convincing evidence of smart de-adhesion was reported. Some other models [11, 18] also used the idea of replacing the seta with compliant spring for simulation, but Johnson-Kendall-Roberts (JKR) theory was chosen to calculate the adhesion force between the spherical tip of seta and flat surface.

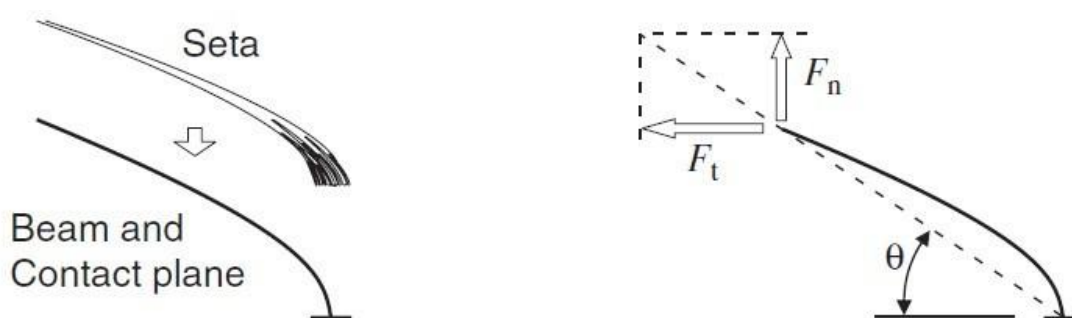
Some other models, especially during the analysis of synthetic microfibers with a canted angle, represented individual seta as an elastic beam [8, 14, 15]. For instance, in ref [8], Lee et al. built their model as an angled microfiber that slides under pure shear load. With one end fixed, the microfiber undergoes bending due to the shear sliding load in either direction along or against the microfiber, as shown in Figure 1.4(b). Similar approaches were used in some other simulations but different boundary conditions and material properties were applied. Using theories of beam bending, buckling, compression and extension, the properties of synthetic adhesives were able to be predicted and compared with experimental results. Some models were even developed to determine the optimal geometry of the microfiber [8, 14]. It was noticed that most of literature used DMT- or JKR-theory-based point contact to treat



(a) Multiple discrete linear springs model (*Bhushan, 2007*)



(b) Individual seta model with a canted angle using elastic beam theory (*Lee 2008*)



(c) Individual seta model with a finite width tip that would impart a moment at the contact surface (*Takahashi 2006*)

Figure 1.4: Several computational models for gecko setae

the interaction between the seta tip and the surface, but none of them provided full explanation for geckos' great reversibility and controllability.

An alternative view of the contact mechanics provided by Takahashi [17] proposed that the seta has a finite width and would impart a moment at the contact surface, as shown in Figure 1.4(c). In this case, the moment generated by the oblique angle during bending would help geckos pry rather than pull apart the contact surface when de-adhering, which could contribute to geckos' smart adhesion ability. However, no detailed model was built or analyzed until now.

This work revealed the central role the canted seta angle plays for a flexible seta, and evaluated the enhancement it makes to the adhesion system. Using Takahashi's idea, the contact between the seta and the surface is assumed to be cohesive so moment can be endured. Two models were built including a heuristic model which focuses on the robustness of adhesion under dynamic load conditions, and a more mature model which applies correct boundary conditions, aiming to find the optimal geometric parameters for geckos to become most efficient and to de-adhere smartly.

1.6 REFERENCES

- [1] J. Mongeau, B. McRae, A. Jusufi, P. Birkmeyer, A. M. Hoover, R. Fearing, and R. J. Full, *Rapid Inversion: Running Animals and Robots Swing like a Pendulum under Ledges*. (2012). Paper 3.
http://digitalcommons.olin.edu/facpub_2012/3
- [2] K. Autumn, *American Scientist*. **2**, 124-132 (2006). *How Gecko Toes Stick*

- [3] K. Autumn, M. Sitti, Y. A. Liang, A. M. Peattie, W. R. Hansen, S. Sponberg, T. W. Kenny, R. Fearing, J. N. Israelachvili, and R. J. Full, *Proc Natl Acad Sci.* **99**, 12252–12256 (2009). *Evidence for van der Waals adhesion in gecko setae*
- [4] K. Autumn, and A. M. Peattie, *Integrative and Comparative Biology.* **42**, 1081-1090 (2002). *Mechanisms of Adhesion in Geckos*
- [5] D. J. Irschick, B. Vanhooydonck, A. Herrel, and A. Andronescu, *The Journal of Experimental Biology.* **206**, 3923-3934 (2003). *Effects of loading and size on maximum power output and gait characteristics in geckos*
- [6] T. W. Kim, and B. Bhushan, *J. Adhesion Sci. Technol.* **21**, No. 1, pp. 1–20 (2007). *Adhesion analysis of multi-level hierarchical attachment system contacting with a rough surface*
- [7] T. W. Kim, and B. Bhushan, *Ultramicroscopy.* **107**, 902-912 (2007). *Effect of stiffness of multi-level hierarchical attachment system on adhesion enhancement*
- [8] J. Lee, R. S. Fearing, and K. Komvopoulos, *Appl. Phys. Lett.* **93**, 191910 (2008). *Directional adhesion of gecko-inspired angled microfiber arrays*
- [9] L. Ge, S. Sethi, L. Ci, P. M. Ajayan, and A. Dhinojwala, *Proc Natl Acad Sci.* **104**, 10792–10795 (2007). *Carbon nanotube-based synthetic gecko tapes*
- [10] N. Gravish, M. Wilkinson, and K. Autumn, *J. R. Soc. Interface.* **5**, 339–348 (2008). *Frictional and elastic energy in gecko adhesive detachment*
- [11] M. Sitti, and R. Fearing, *J. Adhesion Sci. Technol.* **17**, No. 8, 1055-1073 (2003). *Synthetic gecko foot-hair micro/nano-structures as dry adhesives*

- [12] J. Tamelier, S. Chary, and K. L. Turner, *Langmuir*. **28**, 8746–8752 (2012).
Vertical Anisotropic Microfibers for a Gecko-Inspired Adhesive
- [13] H. E. Jeong, J. Leeb, H. N. Kima, S. H. Moon, and K. Y. Suh, *Proc Natl Acad Sci*. **106**, 5639-5644 (2009). *A non-transferring dry adhesive with hierarchical polymer nano-hairs*
- [14] B. Aksak, M. P. Murphy, and M. Sitti, *Langmuir*. **23**, 3322-3332 (2007).
Adhesion of Biologically Inspired Vertical and Angled Polymer Microfiber Arrays
- [15] T. Kim, H. E. Jeong, K. Y. Suh, and H. H. Lee, *Advanced Materials*. **21**, 2276–2281 (2009). *Stooped Nanohairs: Geometry-Controllable, Unidirectional, Reversible, and Robust Gecko-like Dry Adhesive*
- [16] B. Bhushan, A. G. Peressadko and T. Kim, *J. Adhesion Sci. Technol.*. **20**, 1475–1491 (2006). *Adhesion analysis of two-level hierarchical morphology in natural attachment systems for ‘smart adhesion’*
- [17] K. Takahashi, J. O. L. Berengueres, K. J. Obata, and S. Saito, *International Journal of Adhesion & Adhesives*. **26**, 639-643 (2006). *Geckos’ foot hair structure and their ability to hang from rough surfaces and move quickly*

2 BACKGROUND THEORY

It was shown in the introduction that the van der Waals force is central to the geckos adhesion. Due to the relatively large scale (μm) of an individual seta, the geckos adhesion problem is in essence a problem of interaction between macroscopic objects under microscopic interactional force. The Hamaker approach [1], also called the microscopic approach, is effective to address such problems, as introduced in the following section.

2.1 MICROSCOPIC/HAMAKER APPROACH

For the interaction between two molecules, Figure 2.1 shows clearly the force response curve, which is the combination of van der Waals attractive force and short range Coulomb repulsive force. However, in the case of an individual seta, due to relatively large dimensions ($\mu\text{m} \gg 2 \text{ nm}$), the short range Coulomb repulsive force is ignored. Therefore, only the attractive interaction force is discussed in this approach.

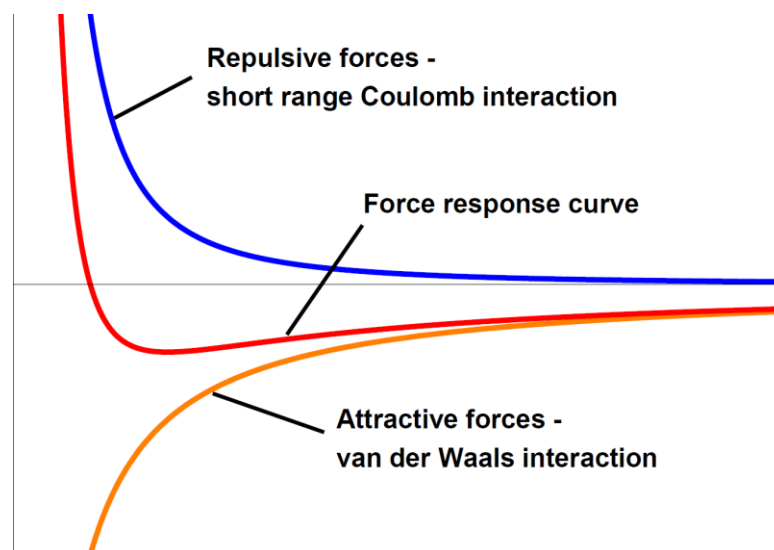


Figure 2.1: Force response curve

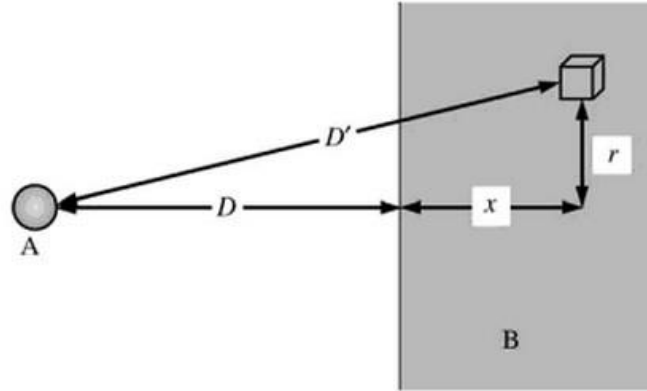


Figure 2.2: Interaction between a molecule and an infinite solid (*Butt et al. 2010*)

For macroscopic objects with known volumes and material properties, the surface van der Waals force can be computed as the sum over all interacting pairs. For instance, as illustrated in Figure 2.2, the van der Waals energy between a molecule A and an infinite solid with a planar surface made of molecules B is computed by integration of the molecular density, Q_B , over the entire volume of the solid, represented as:

$$V_{mol/plane} = -C_{AB} \iiint \frac{Q_B}{D'^6} dV = -C_{AB} Q_B \int_0^{\infty} \frac{2\pi r dr dx}{[(D+x)^2 + r^2]^3},$$

where C_{AB} is a material-dependent constant. In the same way it is possible to calculate the van der Waals energy between two objects with different shapes. In 1937 Hamaker announced a famous equation in his original publication for the approximation of the van der Waals energy between two spherical bodies,

$$V = -\frac{H}{6} \left[\frac{2R_1 R_2}{d_{cc}^2 - (R_1 + R_2)^2} + \frac{2R_1 R_2}{d_{cc}^2 - (R_1 - R_2)^2} + \ln \left(\frac{d_{cc}^2 - (R_1 + R_2)^2}{d_{cc}^2 - (R_1 - R_2)^2} \right) \right],$$

where H is the Hamaker constant which is dependent on material properties for both interacting objects, d_{cc} is the distance between the centers of the spheres, $d_{cc} = D + R_1 + R_2$. If the spheres are significantly large in radii compared to the distance between them, then the equation can be simplified to

$$V(D) = -\frac{H}{6D} \frac{R_1 R_2}{R_1 + R_2}.$$

The van der Waals force is the negative derivative of the potential energy function,

$$F(D) = -\frac{dV}{dD} = -\frac{H}{6D^2} \frac{R_1 R_2}{R_1 + R_2}.$$

For a sphere and a planar surface, the energy and force can be obtained by making one of the radii infinite so $V(D) = -\frac{HR}{6D}$ and $F(D) = -\frac{HR}{6D^2}$.

2.2 GECKOS ADHESION FORCES

Based on the van der Waals formalism, nowadays there are two widely applied theories in the calculation of the adhesion force, f_{ad} , between spatula tips and a surface. The first one is the Derjaguin-Muller-Toporov (DMT) theory [2], which is based on the van der Waals surface forces between two spheres. It can be represented as:

$$f_{ad} = 2\pi R_c E_{ad},$$

where R_c is the radius of contact, which is calculated as $R_c = (1/R_1 + 1/R_2)^{-1}$, where R_1, R_2 are radii of contacting surface; E_{ad} is the work of adhesion per unit area between two infinite bodies with parallel planar surfaces, which is calculated as $E_{ad} = -\frac{H}{12\pi D^2}$. In Bushan's work, the assumption of $R_1=R_2$ is made and the magnitude of R is taken as 50 nm; the typical value of Hamaker constant is taken as 10^{-19} J for β -keratin; D is set as 0.2 nm. As results, the calculated adhesion force is approximately 10 nN per contact (spatula), which is claimed being identical to the experimental measurement for a single spatula [2]. The second theory, called Johnson–Kendall–Roberts (JKR) theory, is based on the van der Waals surface interaction forces between a sphere and a planar surface. It has a similar form to DMT but with its coefficient modified to 3/2. It is represented as:

$$f_{ad} = \frac{3}{2}\pi R_c E_{ad}.$$

Autumn et al. uses JKR theory to predict radii of individual spatula [3]. The adhesion force is measured as approximate 40 uN per seta on a MEMS surface, and the adhesion energy is taken as 50-60 mJ/m² for van der Waals forces. As results, the predicted radii for individual spatulae are around 0.13-0.16 um, which is claimed as being close to empirical measurements. However, neither of their works is accurate enough. In Bushan's work the separation distance is set as 0.2 nm, which is so small that the short range Coulomb repulsive force should be taken into consideration, while in Autumn's work the spatulae are assumed to be tightly packed so the

adhesion stress is applied instead of adhesion force between single spatula and the surface, which could make the predicted radii larger than the actual value.

2.3 COHESIVE CONTACT ASSUMPTION IN THIS STUDY

The dimensions of geckos' hierarchical structure vary with different species. For *Tokay gecko* specifically, the seta is around 30-130 μm in length and 5-10 μm in diameter while the spatula is around 2-5 μm in length and 0.1-0.2 μm in diameter [2]. Empirical data shows that each seta contains 100-1000 spatulae. In this study, for an individual seta, the assumption of tightly packed spatulae is made so the contact between the seta tips and a flat surface is treated as cohesive, as illustrated in Figure 2.3. Each spatula would be able to generate a small amount of adhesion force, and then with the work of hundreds of these tiny structures located on the seta, the adhesive stress could go up to several newtons per square millimeter (1-3 N/mm^2). Furthermore, by changing the contact area (through seta bending, twisting, or number of contacting spatula) and the separation distance, it is steerable to control the magnitude of adhesion stress, even partially. Therefore, the assumption of cohesive contact is reasonable and effective, especially for the adhesion criteria that will be discussed later.

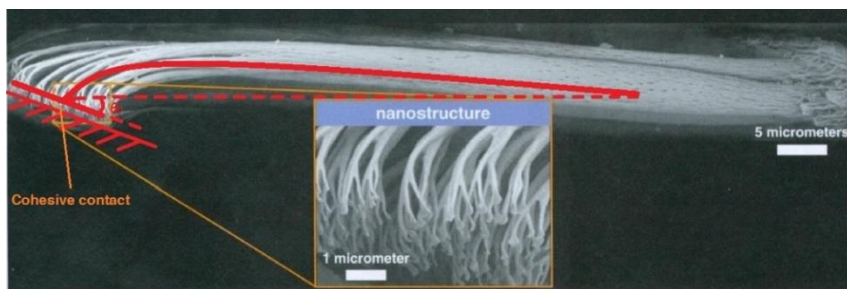


Figure 2.3: Cohesive between seta tips and flat surface.

2.4 REFERENCES

- [1] H. Butt, and M. Kappl, “Surface and Interfacial Forces”, 1st ed. Wiley-VCH, Weinheim GER (2010).
- [2] T. W. Kim, and B. Bhushan, J. Adhesion Sci. Technol.. Vol. 21, No. 1, pp. 1–20 (2007). *Adhesion analysis of multi-level hierarchical attachment system contacting with a rough surface*
- [3] K. Autumn, M. Sitti, Y. A. Liang, A. M. Peattie, W. R. Hansen, S. Sponberg, T. W. Kenny, R. Fearing, J. N. Israelachvili, and R. J. Full, Proc Natl Acad Sci. 99: 12252–12256 (2009). *Evidence for van der Waals adhesion in gecko setae*

3 MANUSCRIPT

Role of Seta Angle and Flexibility in Geckos Adhesion Mechanism

Congcong Hu¹; P. Alex Greaney², M.S.

To be submitted to

Journal of Applied Physics

¹M.S. Candidate, School of Mechanical, Industrial and Manufacturing Engineering, Oregon State University, Corvallis, OR 97331. Email: huc@onid.orst.edu

²Assistant Professor, School of Mechanical, Industrial and Manufacturing Engineering, Oregon State University, Corvallis, OR 97331. Email: alex.greaney@oregonstate.edu

3.1 ABSTRACT

A model is developed to describe the reversible nature of gecko dry adhesion. The central aspect of this model is that the seta can be easily peeled away from the contacting surface by a small moment at the contact tip. It is shown that this contact condition is very sensitive, but can result in robust adhesion if individual seta are canted and highly flexible. In analogy to the “cone of friction”, we consider the “area of adhesion” — the domain of normal and tangential forces that maintain adhesion. Results demonstrate that this adhesion region is highly asymmetric enabling the gecko to adhere under a variety of loading conditions associated with scuttling horizontally, vertically and inverted. Moreover, under each of these conditions there is a low energy path to de-adhesion. In this model obliquely canted seta (as possessed by geckos) rather than vertically aligned fibers (common in synthetic dry adhesive) provide the most robust adhesion.

3.2 INTRODUCTION

Geckos are one of the most specialized climbers in nature having evolved a dry-adhesive that enables them to stick to almost all materials. Their ability to adhere comes from the van der Waals force from millions of branching hairs (setae) on the geckos' feet conforming to the contours of the surface [1-3]. The setae are just one part of a hierarchical adhesion system that maximizes surface contact area, even on fractally rough surfaces, and enables robust load sharing [4-6]. More importantly from the gecko's point of view, this is a smart adhesion system that provides highly reversible traction under a wide range of loading conditions — permitting geckos not just to stick but to also unstick rapidly, and enabling them to run at speeds of up to

twenty body-lengths per second. Since the origin of gecko's adhesion was unequivocally resolved in 2002 [2], numerous groups have sought to create synthetic dry-adhesive tapes patterned with arrays of compliant micro-fibers or pillars that can replicate the phenomenon [7-12]. Development of these synthetic gecko adhesives has revealed a lot of the subtlety employed by real geckos. Recent studies have identified anisotropy of setae as a key feature necessary for smart or reversible adhesion [11, 13]. Motivated by this, the latest generations of synthetic adhesives have explored a variety of strategies to create systematic anisotropy. These include presetting a seta at a canted angle [9-11], using hybrid materials, and modifying the tip shape [7, 9], or vertical symmetrical micro-fibers [8, 12]. These synthetic dry-adhesives have shown remarkable performance in certain desirable aspects; however, they still have a long way to go to match the performance of geckos themselves.

There are two major differences between synthetic dry-adhesives and gecko adhesion. First, many synthetic adhesives possess only one level of hierarchy (due to the complexity in the fabrication), while the gecko possesses an adhesion system with multiple levels of hierarchy spanning from its four feet, through toes, lamellae, to setae that branch three times at their tips. Second, many synthetic adhesives have fibers oriented vertically, while the gecko's setae are canted at an oblique angle. Computational models have been powerful for understanding the effect of these differences. Among these models, a discrete linear springs model by Bhushan explains the adhesion enhancements afforded by hierarchically branched setae [14, 15]. Other models have represented individual seta as elastic beams in order to

determine the optimal geometry for synthetic setae [10-12, 16]. Both types of model have treated the seta tip as a point contact, and neither has provided a full explanation of smart de-adhesion. One mechanism for easy de-adhesion has been proposed by Takahashi who noted that setae have a finite width and would impart a moment at the contact surface [17], as shown in Figure 3.1(a). This could be used by the gecko to pry rather than pull apart the contact between seta tips and an adhering surface. This is a compelling idea; however, no detailed model was built or analyzed until now.

In this work we elucidate the central role that the combination of canted flexible setae play both for adhesion and in Takahashi's mechanism for easy de-adhesion. We present several models of adhering seta — the feature that distinguishes these from previous models is that the seta's contacting tip is able to support a moment. The first model is heuristic and demonstrates that flexibility of the seta is crucial for providing robustness of adhesion under dynamic loads while the moment enables easy de-adhesion. The final model is representative of a gecko's seta and we use it to determine geometric parameters that would be optimal for the gecko.

3.3 HEURISTIC MODEL

3.3.1 Moment-supporting Contact

The oblique seta angle has been proposed as the key factor for geckos' ability to easily unstick when they are walking or climbing. In order to explore the interplay of this canting angle with the soft compliance of a seta, a basic single seta model is constructed, as is shown in Figure 3.1(b). As is seen in Figure 3.1(a), real seta have

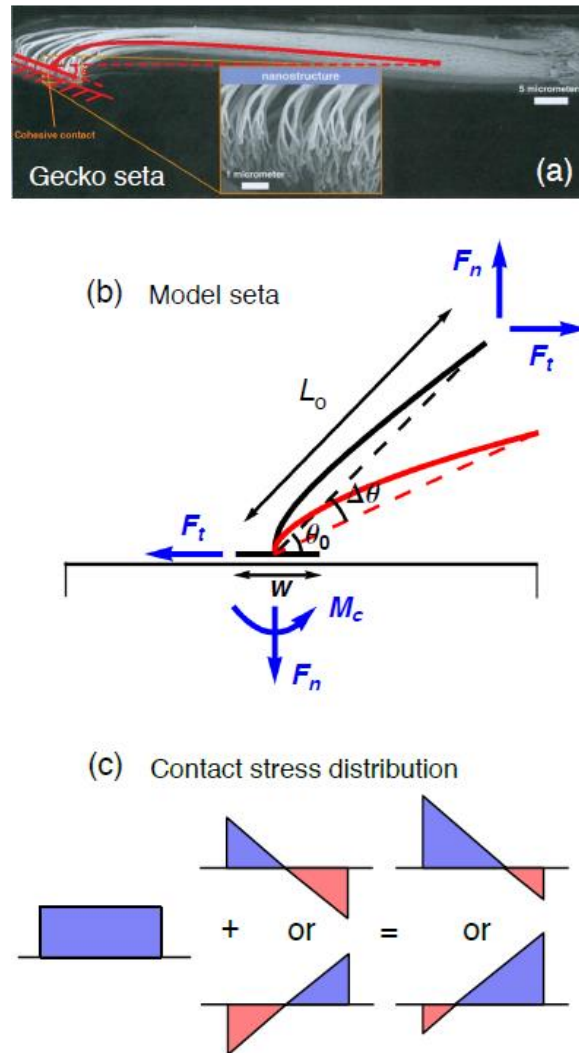


Figure 3.1: Heuristic model and adhesion criterion. (a) Scanning electron micrograph of a *Tokay* gecko (*Gekko gecko*) seta overlaid with a depiction of the model seta geometry considered in this work. The micrograph was taken by Keller Autumn and originally published in ref. [1] and is reproduced with the kind permission of the author. (b) Schematic of a seta contacting a surface and supporting normal and tangential forces F_n , and F_t . (c) Shows the normal stress distribution in the contacting pad due to a combination of the normal force F_n and the moment M_c at the contact. In this model de-adhesion occurs when any portion of the stress distribution exceeds the tensile adhesion limit σ_{ad} .

branched tips ending in an array of small contacts. In our model we ignore the details of the branching and represent the array of contacts with a single planar contact pad that feels a non-uniform adhesive stress. The result is that the contact can support a small moment and that the contact moment can greatly affect the peak stress in the contact. We assume there to be a limiting stress, σ_{ad} , for adhesion, and if any part of the contacting area exceeds this limiting stress the seta de-bonds from the surface. Thus, as is shown in Figure 3.1(c), the strength of the seta's adhesion is dependent not just on the normal load, but is also sensitive to the moment at the contact. This setup was first proposed by Takahashi [17] — it provides a mechanism to easily peel or pry off the contact when unsticking. The condition for adhesion is very sensitive to the moment M_c at the contact requiring the horizontal and vertical loads on the seta to be carefully balanced to during adhesion. In this work we do not impose any limit to the tangential forces. There will clearly be a critical shear stress that causes the seta to slide, however this can be added without altering the mechanics of de-adhesion and so we omit it from the present calculations and consider its effect at the end.

The seta is taken to have a canting angle θ , that is, the angle from the base of the seta to the contact ignoring the seta's curvature. The distal contact feels adhesion forces tangential, F_t , (positive towards the gecko) and normal, F_n , to the surface. As stated in Ref. [17], when $\frac{F_n}{F_t} = \tan(\theta)$, the moment imparted on the tip becomes zero and the normal stress is flat, distributed as shown in the leftmost figure in Figure 3.1(c). However, if the seta contact can support a small moment then these forces become decoupled and the moment at the contact, M_c , is given by:

$$M_c = LF_t \sin(\theta) - LF_n \cos(\theta), \quad (1)$$

where L is the distance from the contacting tip to the seta's root, indicated in Figure 3.1(b). The moment at the contact depends only on the forces at the seta's root and the position of the root. In this heuristic model we assume the seta's root to be free to move and also to rotate. As can be seen in Figure 3.1(c), the combination of a flat stress distribution generated by the normal force (left) with symmetric triangular stress distribution generated by the moment (middle) results in a non-uniform asymmetric stress distribution with the maximum normal stress on the edge given by:

$$\sigma_{\max} b = \frac{6|M_c|}{w^2} + \frac{F_n}{w}, \quad (2)$$

where w is the contacting width of the contact pad shown in Figure 3.1(b), and b is the thickness of the pad into the page. In this article we will consider dimensionless versions of the forces f and moment m that we define as fractions of the pull of force: $f = \frac{F}{\sigma_{ad}wb}$, and $m = \frac{M_c}{L_0\sigma_{ad}wb}$, where L_0 is the undeformed length of the seta (in this model we impose that $L = L_0$ but in the later model this condition is relaxed). Using Eq.2 with the adhesion criterion $\sigma_{ad} > \sigma_{\max}$ gives an upper and lower value for the dimensionless moment at the seta contact at detachment

$$1 = fn \pm 6\lambda m_c \quad (3)$$

where $\lambda = L_0/w$ is the seta aspect ratio. These equations bound the set of loading conditions, f_n and f_t , for which the seta will remain stuck to the surface. If the seta remains rigid then the dimensionless “adhesion region” is a slender oblique triangular wedge with width dictated by the aspect ratio λ . From Figure 3.1(a) we estimate this aspect ratio to be in the range of 8–12 (we used 10 for the calculations reported here), which results in a very narrow adhesion region demarked by dashed lines in Fig.2(a). Importantly, the adhesion region is asymmetric. To resist a large normal load the gecko must supply a moment balancing tangential force inward (in a proximal direction). This asymmetry means that to easily de-adhere the gecko need only remove the tangential force. Clearly the loads f_n and f_t on a seta will be very different depending on whether the gecko is running on a horizontal surface, climbing vertically or hanging inverted. Moreover, the f_n/f_t ratio will differ dramatically as the gecko loads and unloads the seta, and will also differ between neighboring seta. Most surfaces are rough and so the contact conditions vary from seta to seta. Performing dynamic motion while maintaining the majority of setae adhered to the surface will require a very broad set of adhesion conditions. The key to this is the ability of the seta to bend.

3.3.2 Flexible Seta

Under unbalanced loads the seta will bend in the direction that reduces the lever arm of the dominant load (and increasing the lever arm of the weaker force) and will thus buffer the effects of unbalanced moments from f_n and f_t . We model the flexural behavior of the seta as a torsional spring with dimensionless stiffness, k , such that

$k\Delta\theta = m_c$. The net dimensionless bending moment at the contact, m_c , is then a nonlinear function of the loading and is given by

$$m_c = f_t \sin(\theta_0 + \Delta\theta) - f_n \cos(\theta_0 + \Delta\theta), \quad (4)$$

where θ_0 is the preset angle, i.e., the canting angle of the un-deformed seta. The adhesion condition in Eq.3 still holds. We compute the adhesion regions by solving Eqs.3 and 4 numerically to find the f_t and $\Delta\theta$ at the adhesion limit for a given value of f_n .

Figure 3.2(a) shows the adhesion regions for a flexible seta with preset angles of 45° and 30° (both with the for same dimensionless stiffness $k = 0.0375$). Allowing the seta to bend greatly expands the adhesion region. While the adhesion region remains narrow for small f_n and f_t , under large loads adhesion is robust to a wide range of load ratios f_n / f_t .

Marrying robustness of seta adhesion (a wide adhesion region) with easy de-attachment (asymmetric adhesion region) is essential for the gecko. In the gecko adhesion system, each seta does not work in isolation, but experiences a range of loads depending on the behavior of adjacent setae and its adhering to rough surfaces.

As a simple first metric of this we consider the radius of loading space (*i.e.* the scatter in) f_n and f_t that the seta can tolerate and still remain stuck. This is quantified by finding the radius of the largest circle that can fit in the adhesion region. Figure 3.2(b)

shows the plot of this radius as a function of canting angle for setae of different stiffnesses. While this metric has no rigorous theoretical foundation it provides a completely objective metric that we can use to compare different seta geometries. It can be seen that orienting the seta with a more oblique angle greatly increases the width of the adhesion region, as does increasing seta flexibility.

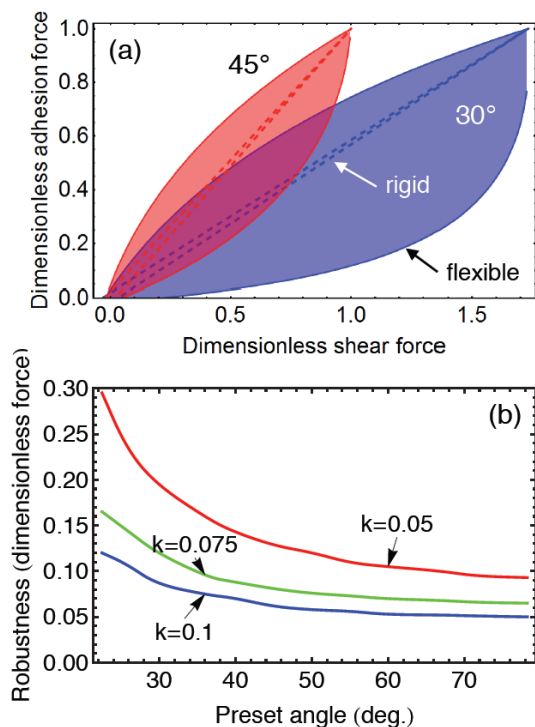


Figure 3.2: Adhesion region and robustness plots. (a) Dimensionless adhesion region of flexible and rigid seta computed with preset canting angles of $\theta_0 = 45^\circ$ (red) and $\theta_0 = 30^\circ$ (blue). In all cases $\lambda = 10$. The flexible seta were computed with $k = 0.0375$. Allowing the seta to bend massively increases the adhesion region by deforming to reduce moments at the seta contact. (b) Plots of the dimensionless robustness, which is quantified in units of dimensionless force (see text for details), for seta with varying dimensionless stiffness as a function of the preset canting angle.

In this model for dry adhesion, the resistance to tensile normal force results from an applied tangential force. It is instructive to make the comparison between the gecko adhesion and static friction as these are in many ways opposites (see Figure 3.3). Static friction creates resistance to sliding forces as the result of a compressive normal force. The gecko's dry adhesion is able to resist a tensile normal force as a result of a tangential force. In order to generate adhesion the gecko must press and slide its feet towards its body. This process enables setae to make intimate surface contact, however, we propose that this dragging also acts to balance moments that would otherwise peel away the setae contacts.

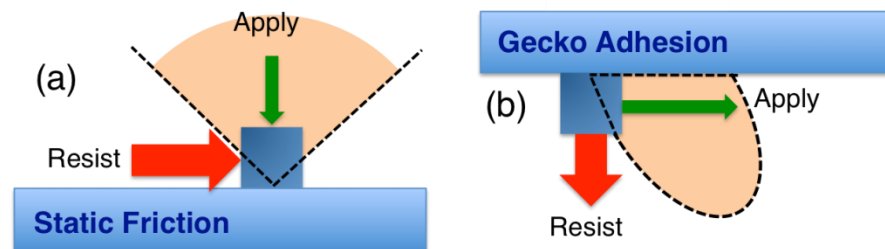


Figure 3.3: Schematic contrasting geckos' dry adhesion with static friction. (a) Friction provides resistance to a shear force as a result of a compressive normal force. If the total force vector is anywhere inside the cone of friction, the interfaces will remain static. (b) Geckos resist a tensile normal load through the application of a shear force. The resulting force must lie inside the adhesion region for the joint to remain stuck. In contrast to friction, the adhesion region must be asymmetric to provide easy de-attachment.

While our very simple heuristic model demonstrates that the combination of flexibility and oblique preset in moment supporting setae provides an advantage for adhesion, clearly there must be an optimal limit for each of these attributes. Setae that are too long or flexible will become matted and entangled with each other. If setae are too close to horizontal the gecko must apply a huge tangential force to balance a moderate normal force. This will either result in setae sliding, or as biological motors require energy just to exert a static force, it will mean the gecko has to exert a lot of energy to adhere. All of these phenomena are excluded from our simple model but they allow us to identify the tradeoffs in the evolutionary optimization of geckos' adhesion system. Setae must be stiff enough to creating a non-matting array with large area density. They must be moderately canted to permit easy de-adhesion while only requiring moderate shear force from the gecko to hold a large normal force. Moreover, the gecko must be able to climb vertically as well as hang upside down — so a gecko's foot must be able to support a large tangential force with little normal force.

To explore methods to broaden the adhesion region in the simple model we consider the effect of nonlinearity in the seta's flexibility. Real seta has a curved and branched structure and undergoes large deformations. Thus it is reasonable to expect that the bending stiffness is nonlinear and asymmetric. To capture this we replace the dimensionless linear bending stiffness with a nonlinear stiffness function,

$$k_{nl} = k_1 + k_2 \frac{\Delta\theta}{\theta_0} + k_3 \left(\frac{\Delta\theta}{\theta_0} \right)^2, \quad (5)$$

where k_2 and k_3 are the first asymmetric and symmetric nonlinear stiffness terms. Positive k_2 stiffens the seta when it is bent down, and positive k_3 stiffens the seta under large deflections in either direction. The adhesion region of non-linear seta is shown in Figure 3.4. Very flexible seta provides a large and robust adhesion region with the limiting case of a perfectly flexible seta being equivalent to a point contact, with no easy path for de-adhesion. The design rationale for non-linear stiffness is then to obtain a broad range of motion for the seta with little contact moment, but for the seta to stiffen outside of this range resulting in rapid detachment. Figure 3.4 demonstrates that only including a positive k_3 term can result in a large expansion of the adhesion region while still providing a route for easy unsticking.

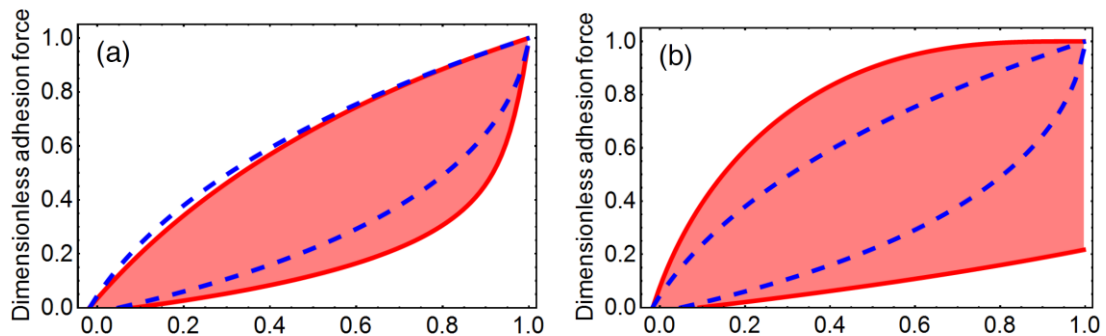


Figure 3.4: Plot of the adhesion region for seta with nonlinear bending stiffness (red) overlaid with the adhesion region for linear seta (blue). Plot (a) is computed with $k_1 = 0.0375$, $k_2 = 1$, and $k_3 = 1$. Plot (b) is computed with $k_1 = 0$, $k_2 = 0$, and $k_3 = 1$. In both (a) and (b) the blue overlaid curve is computed with $k_1 = 0.0375$, $k_2 = 0$, and $k_3 = 0$. In all cases $\lambda = 10$, and $\theta_0 = \pi/4$.

3.4 GECKO MODEL

3.4.1 Gecko Model Setup

To further explore the mechanism for detachment we consider the energy stored in the seta and the work of de-adhesion for various loading paths. The heuristic model is overly simplistic and includes no linear extension of the seta. This means that it would require no work to detach the seta if the force is applied along θ_0 . To correct this we consider a second model that is more representative of the Gecko and that permits us to examine work of de-adhesion. This model has two significant differences, firstly it assumes that the seta is extensible, and secondly that they support a moment both at its tip, and at its root where it joins the gecko's foot, as shown in Figure 3.5(a). We impose the boundary condition that as the seta flexes the contact pad must remain horizontal to stay bonded to the surface. This gives the condition that $\alpha_f + \alpha_m = 0$, where α_f , and α_m are the rotation angle of the seta tip due to bending force, $(F_t L \sin(\theta) - F_n L \cos(\theta))$, and a moment M_c , respectively. We consider the seta as a curved beam with a varying moment of inertia and modulus, and we show that this geometry can be mapped to a simpler system of two torsional springs as shown in Figure 3.5(b). In elastic beam theory the bending angle from the base of a cantilevered beam to its tip ($\Delta\theta$) scales linearly with the rotation angle at the free end (α) and can be expressed as $\frac{\alpha_f}{\Delta\theta_f} = \beta_f, \frac{\alpha_m}{\Delta\theta_m} = \beta_m$. Geometrically the ratios β must satisfy $\beta_m > \beta_f > 1$. (To provide some physical context for interpreting these geometric parameters we note that β_f and β_m for a simple cantilever beam are 1.5 and 2 respectively.) The compatibility condition leads to the expression for the dimensionless moment at the contacting tip,

$$m_c = \frac{k_m \beta_f}{k_f \beta_m} (f_n \cos(\theta) - f_t \sin(\theta)), \quad (6)$$

where k_f and k_m are the dimensionless angular stiffness of the seta as a whole in response to a moment m_g at the seta root imparted by either a bending force or a moment, respectively, applied at the seta tip. Note also that geometrically k_f must be larger than k_m . From the balance of moments, this gives the ratio of contact to root moments

$$\frac{m_c}{m_g} = \frac{k_m \beta_f}{k_f \beta_m - k_m \beta_f}. \quad (7)$$

For a seta modeled as a curved beam the values of k_f , k_m , β_f , and β_m can be found from elementary mechanics using the unit load method. However, with the imposed boundary condition of zero net contact rotation, then we can find an equivalent two-torsional-spring system as depicted in Figure 3.5(b) with $k_c = \frac{k_m \beta_f}{\beta_m - \beta_f}$ and $k_g = \frac{k_f \beta_m - k_m \beta_f}{\beta_m - \beta_f}$. that undergoes the same displacement and possesses the same moment ratio as the geometry-based model for a given loading condition. In this simpler system $\Delta\theta = \frac{m_c}{k_c} = \frac{m_g}{k_g}$ and

$$\frac{m_c}{m_g} = \frac{k_c}{k_g} = \eta. \quad (8)$$

This means that the system response is described by an effective root stiffness k_g and stiffness ratio η . Thus, rather than estimating k_f , k_m , β_f , and β_m for seta shaped beams (which would contain much uncertainty) we determine the stiffness scale and ratio η that is optimal for the gecko. We leave the problem of identifying beam geometries with the desired η for later research.

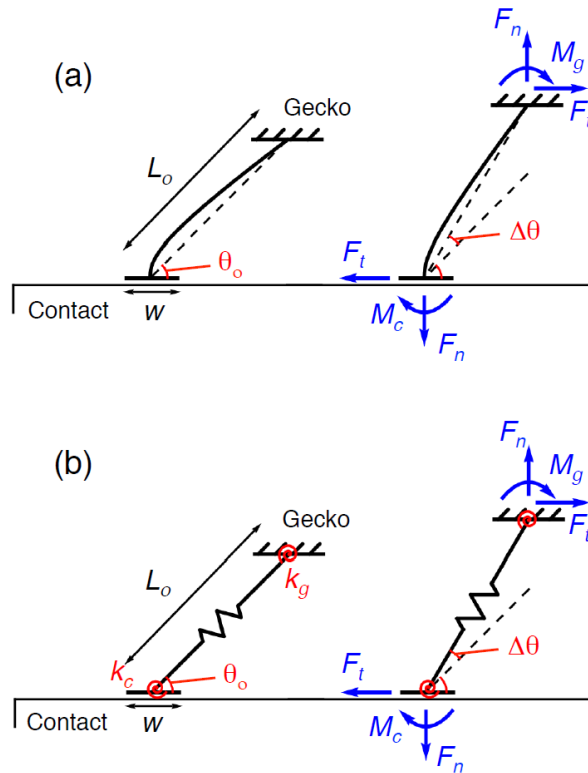


Figure 3.5: Gecko model. (a) shows the schematic of a real gecko seta. The seta is cantilevered from its root and bends under the actions of bending forces (F_t and F_n give rise to bending force $F_t L \sin(\theta) - F_n L \cos(\theta)$) and moments (M_c) applied at its tip. While adhered to a surface the contact pad is must be rotated parallel to the surface. (b) shows the beam like model of a seta from (a) mapped to a system of two torsional springs (k_c and k_g). In both (a) and (b) the left hand figure shows the undeformed seta and the right hand side the seta supporting a load.

Finally, tensile stiffness k_t is included to model elongation of the seta. The resulting contact moment is given by

$$m_c = (1 + \varepsilon)(f_t \sin(\theta) - f_n \cos(\theta)), \quad (9)$$

with $\theta = \theta_0 + \Delta\theta$, and the fractional elongation, ε , given by

$$\varepsilon = \frac{1}{k_t}(f_t \cos(\theta) + f_n \sin(\theta)). \quad (10)$$

As before the limits for adhesion are given by Eq.3.

3.4.2 Gecko Model: Results and Discussion

The two-torsional-spring model has a qualitatively different adhesion region from the simple model as shown in Figure 3.6. The two-spring model supports a much broader range of tangential forces under small normal force and thus provides more robust adhesion particularly during dynamic loading.

The plot in Figure 3.6(c) shows the change in the adhesion region with an increase in tip stiffness k_c (for constant stiffness ratio η), and the effect of reducing the stiffness ratio (for constant k_c). It is clear from these plots that the adhesion region expands with decreasing η , and decreasing k_c , i.e., setae that are flexible but stiffer at their root than at their tip. The density plots in Figure 3.7 show the elastic energy stored in two setae as a function of loading conditions (the elastic energy is indicated by the colored

shading with the thick black line marking the boundary of the adhesion region). Together these plots show that the tensile stiffness of the seta, k_t , plays a negligible role in determining the boundary of the adhesion region, but is important for the elastic energy, particularly under large tensile loads. The curved shape of the gecko's setae makes them relatively soft in tension. Setae elongate by straightening under tensile loads and from the geometry of the seta in Figure 3.1(a) we estimate that k_t is 30–100 times larger than k_c . (This estimation was obtained by computing the extension and bending stiffness of a curved beam using the unit load method.)

The energy maps in Figure 3.7 show that there is a good reason for having setae that are soft in tension. The elastic energy stored in the seta when it breaks free is lost and thus this energy is the work of detachment. The flexibility of a seta results in a large amount of deflection, and thus a large stored bending energy. The stored elastic energy is inversely proportional to the stiffness. If the tensile stiffness is too large relative to torsional stiffness (as in Figure 3.7(a)) the lowest energy route for detachment is under a large f_n and f_t . By reducing the axial stiffness to balance the torsional energy one creates a tougher adhesive. Moreover, there is now an easy low energy pathway for detachment in which the stored elastic energy is recovered. This involves removing the tangential load f_t (imparted by the gecko) before removing f_n . Plot (c) in Figure 3.7 shows the energy map and adhesion region for a soft seta but with increased root stiffness k_g . It can be seen that stiffening the seta root enlarges the adhesion region, but in doing so removes the low energy path for detachment and thus would not be optimal for the gecko. From the maps in Figure 3.7 we see that

there must be an optimal balance of k_c , k_g , and k_t that give the potential for large stored energy (and thus tough adhesion), but tradeoff large adhesion region (and thus robust adhesion) with a low energy de-adhesion path (and thus efficiency for the gecko).

Going beyond calculating the work of de-adhesion, we can consider the work done by f_i and f_n along different pathways to de-adhesion. The dashed contour lines on Figure 3.7 indicate lines of constant horizontal (red) and vertical (blue) displacement of the seta root. Thus for loading or unloading along any of the red contours f_i does no work, and f_n performs no work during loading paths that follow the blue contours. We now consider three loading scenarios and examine potential unloading paths for each.

Case 1: Large f_n and moderate f_i . This loading condition arises when the gecko is walking upside down sticking to inverted horizontal surfaces. The gecko must supply force f_i to stick but gravity supplies f_n . Under these conditions an adhered seta has a large quantity of stored energy. This energy is easily recovered to f_i by an unloading path that follows a blue contour. By recovering the energy to work along f_i the energy is returned to the gecko.

Case 2: Low f_n and f_i . This loading condition arises when the gecko is walking normally on flat surfaces. The gecko requires a low energy, low force, detachment path. This is achieved by a small negative (distal) f_i and f_n . The minimum force for detachment can be reduced by increasing the tip/root stiffness ratio (η) to increase the

anisotropy in the adhesion region at $f_n = 0$. By having canted setae, the default stickiness of the gecko's foot is relatively low. Strong adhesion must be activated by a tangential force

Case 3: Small or moderate f_n and large f_t . This loading condition arises when the gecko is climbing vertical surfaces. The gecko must be able to resist large f_t from gravity with relatively little moment balancing f_n . Under these conditions the gecko has an easy path to de-adhesion by first unloading f_n and then following the path in case 2. To be able to stick while climbing vertically the adhesive needs to provide a large static friction force with a small tensile load. This necessitates an adhesion region that extends along the f_t axis as seen in Figure 7(a–c).

The energy maps in Figure 3.7 provide some insight into why the gecko's adhesion system is so successful. When moving around the gecko wants to expend as little energy as possible and so the gecko needs a pathway in which it can unstick without expending energy. However, when jumping, catching itself, or changing directions quickly to avoid predation, the gecko's adhesion system has to absorb a great deal of energy. Moreover, the gecko's adhesion system needs to be able to provide these different functions across a wide range of orientations — that is, with gravity pointing in different directions. The map in Figure 3.7(b) shows that a seta can perform all of these functions: creating tough adhesion under certain load directions but with unloading paths for de-adhesion that can return most of the stored elastic energy to the gecko. The red and blue contours show that different unloading paths can be used

to return energy as work along either f_n or f_t . This is significant as depending on the gecko's orientation, either f_n or f_t could be supplied by the gecko with the other force component coming from gravity.

The balance of flexibility and extensibility of the seta enables this energy absorption and return to happen at the seta level producing a tough joint with large work of de-adhesion. Although the returned elastic energy will not return to chemical energy in the gecko's muscles it is returned to elastic energy in the gecko's muscular system and so we consider it "recovered". It is beyond the scope of this article to examine the biodynamic and physiology of gecko locomotion but we note that there are other animals that are well known to recover elastic energy in locomotion — most notably the jumping kangaroo. The seta is only one part in the gecko's hierarchical system of adhesion that spans from legs through toes and lamellae to seta and spatulae. Assuming that evolution has created the seta not in isolation but as part of a highly energy efficient system, our work raises the interesting question about how the compliance of the setae is matched to that of the lamellae and the rest of the gecko's physiology in order to utilize energy return. It is interesting that the combined area of setae over a gecko's four feet is sufficient to support approximately 50 times its body weight. We speculate that this limiting force is correlated with some other system level behavior such as the number of Gs other parts of the gecko can sustain, the maximum power output from the gecko's muscles, or the natural resonant frequency of the gecko hanging from its legs.

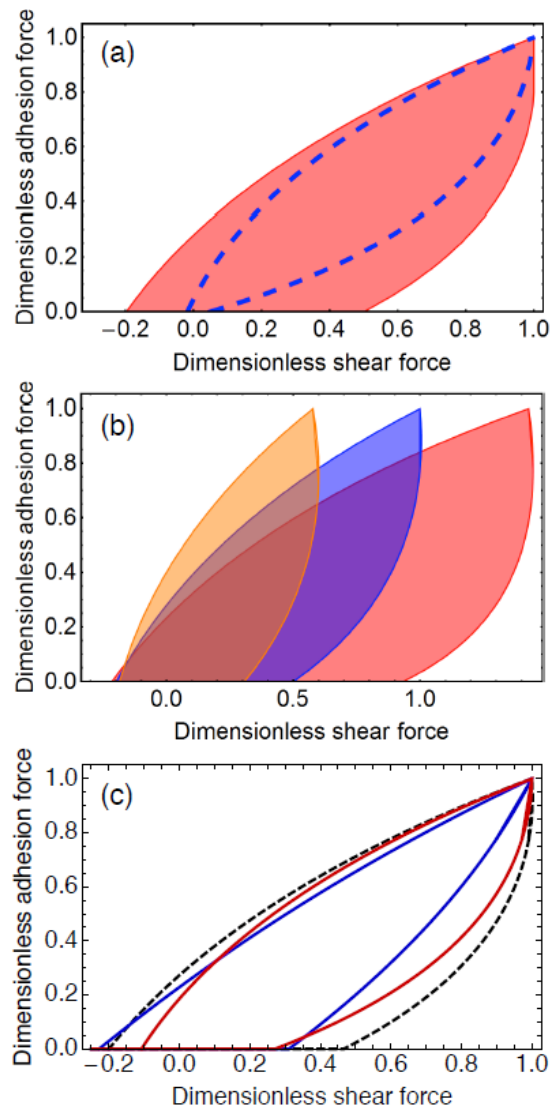


Figure 3.6: Plots of the adhesion region of the two-torsional-spring model. (a) Comparison of the two-torsional-spring model (red) with the single-torsional-spring model (blue). (b) Plots of the adhesion region of the two-torsional-spring model of a seta with preset angles $\theta_0 = 60^\circ$ (orange), $\theta_0 = 45^\circ$ (blue), and $\theta_0 = 35^\circ$ (red). (c) The change in adhesion region for varying η and k_c . The dashed black line is computed with parameters were $\lambda = 10$, $\eta = 0.1$, $k_c = 0.0375$, and $k_t = 5$. The reducing k_g by a factor of two produces the adhesion region plotted in red, and increasing k_c by a factor of two results in the adhesion region plotted in blue.

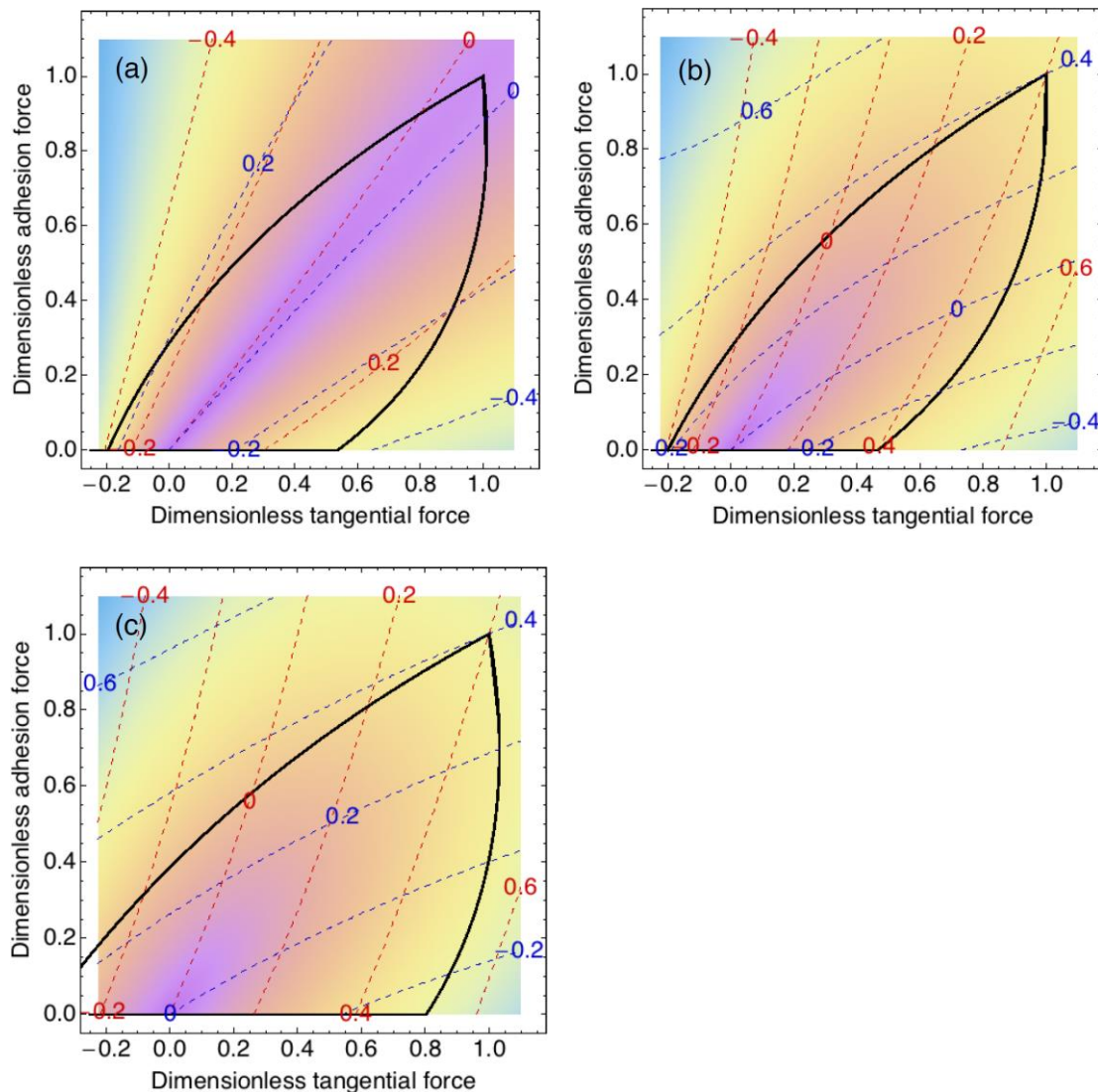


Figure 3.7: Density maps of the stored elastic energy in a seta. Purple and pink indicates no or little stored energy and yellow and blue indicate moderate to large stored energy. The thick black line marks the boundary of the adhesion region and the red and blue dashed lines are contours of constant horizontal and vertical tip displacement, respectively. Plot (a) shows the energy map for a seta with large extensive stiffness, $k_t = 50$, and plot (b) shows the energy for a soft seta with $k_t = 5$. In both (a) and (b) the seta has canting angle $\theta_0 = 45^\circ$, aspect ratio $\lambda = 10$, torsional stiffness ratio $\eta = 0.1$, and dimensionless tip stiffness $k_c = 0.0375$. It can be clearly

seen that changing k_t makes very little difference to the shape of the adhesion region, but dramatically alters the energy landscape. Plot (c) shows the energy for a seta that is soft in tension ($k_t = 5$) as in (b) but with a stiffer root so that the stiffness ratio $\eta = 0.05$. It can be seen that this increases the adhesion region but at the expense of a low energy detachment path. As can be gauged from the deflection contours on all plots our choice of a soft root stiffness $k_g = 0.0375$ is sufficient permit the seta to bend a great deal but the angle of bending does not exceed 30 degrees anywhere in the adhesion region.

3.5 CONCLUSIONS

We have developed two models that explore the mechanism for easy detachment in gecko adhesion. This mechanism is based on the interplay of two processes: moments at the seta contact pry off the seta providing low energy de-adhesion; bending by flexible seta screens the buildup moments at the seta contact and so provides a broad range of loading conditions under which the seta will remain stuck. Central to the interplay of these two processes is that the seta is at an oblique angle. The oblique canting angle has the effect of making the seta in the permanently un-sticky configuration, with adhesion only activated by a moment balancing tangential force supplied by the gecko. Moreover, we show with this simple model that robustness of adhesion can be greatly increased while still possessing easy detachment if the seta has a nonlinear bending stiffness.

Our second, more realistic model of the gecko seta shows that low k_c and low η can produce a large robust adhesion region with a low energy path for unsticking from a

variety of different loading conditions that the gecko might experience during walking, climbing and hanging.

Together the findings from these two models have important ramifications for the development of synthetic dry adhesives. They show that to optimize adhesion synthetic seta must be designed holistically in a way that matches the geometry of the tip with the flexibility and canting angle of the rest of the fiber. Our models show that curved setae increase the toughness of the adhesive, and that creating synthetic setae with nonlinear flexibility could greatly increase robustness of the adhesive.

3.6 ACKNOWLEDGMENTS

This work had benefited from the Extreme Science and Engineering Discovery Environment (XSEDE), which is supported by National Science Foundation grant number OCI-1053575.

3.7 REFERENCES

- [1] K. Autumn, *American Scientist*. **2**, 124-132 (2006). *How Gecko Toes Stick*
- [2] K. Autumn, and A. M. Peattie, *Integrative and Comparative Biology*. **42**, 1081-1090 (2002). *Mechanisms of Adhesion in Geckos*
- [3] K. Autumn, M. Sitti, Y. A. Liang, A. M. Peattie, W. R. Hansen, S. Sponberg, T. W. Kenny, R. Fearing, J. N. Israelachvili, and R. J. Full, *Proc Natl Acad Sci*. **99**, 12252–12256 (2009). *Evidence for van der Waals adhesion in gecko setae*

- [4] N. M. Pugno, and E. Lepore, *BioSystems*. **94**, 218 (2008). *Observation of optimal gecko's adhesion on nanorough surfaces*
- [5] B. Persson, *Surface Science Reports*. **61**, 201-227 (2006). *Contact mechanics for randomly rough surfaces*
- [6] K. Autumn, and N. Gravish, *Philosophical Transactions: Mathematical, Physical and Engineering Sciences*. **366**, 1575-1590 (2008). *Gecko Adhesion: Evolutionary Nanotechnology*
- [7] J. Tamelier, S. Chary, and K. L. Turner, *Langmuir*. **28**, 8746–8752 (2012). *Vertical Anisotropic Microfibers for a Gecko-Inspired Adhesive*
- [8] L. Ge, S. Sethi, L. Ci, P. M. Ajayan, and A. Dhinojwala, *Proc Natl Acad Sci*. **104**, 10792–10795 (2007). *Carbon nanotube-based synthetic gecko tapes*
- [9] H. E. Jeong, J. Leeb, H. N. Kima, S. H. Moon, and K. Y. Suh, *Proc Natl Acad Sci*. **106**, 5639-5644 (2009). *A non-transferring dry adhesive with hierarchical polymer nano-hairs*
- [10] B. Aksak, M. P. Murphy, and M. Sitti, *Langmuir*. **23**, 3322-3332 (2007). *Adhesion of Biologically Inspired Vertical and Angled Polymer Microfiber Arrays*
- [11] J. Lee, R. S. Fearing, and K. Komvopoulos, *Appl. Phys. Lett.* **93**, 191910 (2008). *Directional adhesion of gecko-inspired angled microfiber arrays*
- [12] T. Kim, H. E. Jeong, K. Y. Suh, and H. H. Lee, *Advanced Materials*. **21**, 2276–2281 (2009). *Stooped Nanohairs: Geometry-Controllable, Unidirectional, Reversible, and Robust Gecko-like Dry Adhesive*

- [13] N. Gravish, M. Wilkinson, and K. Autumn, *J. R. Soc. Interface.* **5**, 339–348 (2008). *Frictional and elastic energy in gecko adhesive detachment*
- [14] B. Bhushan, A. G. Peressadko and T. Kim, *J. Adhesion Sci. Technol.* **20**, 1475–1491 (2006). *Adhesion analysis of two-level hierarchical morphology in natural attachment systems for ‘smart adhesion’*
- [15] T. W. Kim, and B. Bhushan, *J. Adhesion Sci. Technol.* **21**, No. 1, pp. 1–20 (2007). *Adhesion analysis of multi-level hierarchical attachment system contacting with a rough surface*
- [16] M. Sitti, and R. Fearing, *J. Adhesion Sci. Technol.* **17**, No. 8, 1055-1073 (2003). *Synthetic gecko foot-hair micro/nano-structures as dry adhesives*
- [17] K. Takahashi, J. O. L. Berengueres, K. J. Obata, and S. Saito, *International Journal of Adhesion & Adhesives.* **26**, 639-643 (2006). *Geckos’ foot hair structure and their ability to hang from rough surfaces and move quickly*

4 CONCLUSION

The geckos adhesion system was studied and the mechanism of easy detachment was explored using two self-developed computational models.

With the canted seta angle and moment imparted on both sides, the models show that geckos would resist a tensile normal load through the application of a shear load, and vice versa. The resulting force combination must lie inside the adhesion region for the joint to remain stuck. The canted seta angle plays a central role in this mechanism. It not only allows the flexible seta to bend but is a prerequisite, with which the adhesion can be only activated by a moment balancing with a tangential force supplied by the gecko.

The first heuristic model shows materials with lower stiffness and geometries with smaller canted angle would be more robust, and are therefore preferred for having the capability to adapt to various load conditions. Introducing non-linear and asymmetric bending stiffness is useful in broadening the adhesion region to further enhance adhesives' reversibility and controllability.

The second more realistic gecko model shows that low k_c and low η can produce a large robust adhesion region with a low energy path for detaching from various loading conditions that geckos might experiencing during walking, climbing and hanging.

Overall, this work reveals the subtle interplay of flexibility and provides new threads for developing enhanced synthetic adhesives with a canting angle. It also suggests for robust adhesion, easy de-adhering is a result of detaching along low energy path.

Several areas for future investigation include:

- Experimentally verify the gecko model;
- Based on the results of this individual seta model, build the hierarchical model which is constructed by multiple setae to explore the effect of collective behavior on the gecko adhesion system.